



# XRD, FT-IR, Electronic and Fluorescence Spectroscopic Studies of Benzothiophenesulfone-2-methanol

<sup>1</sup>Katta Eswar Srikanth, <sup>2</sup>K. Anand Solomon <sup>†</sup><sup>1</sup>A. Veeraiah

<sup>1</sup>Molecular Spectroscopy Laboratory, Department of Physics,  
D.N.R.College (A), Bhimavaram, A.P., India-534202

<sup>2</sup>Department of Chemistry, School of Engineering,  
Dayananda Sagar University, Bangalore-560068, India

<sup>†</sup>Email: [avru@rediffmail.com](mailto:avru@rediffmail.com)

## Abstract

*The structural, vibrational and quantum mechanical properties of Benzothiophene sulfone-2-methanol have been studied on the optimized structure by applying experimental techniques (XRD, FT-IR, UV & Fluorescence) and density functional theory (DFT) employing B3LYP interchange interrelation with the 6-311++G\*\* basis set. Single crystals of the title compound have been prepared with methanol as a solvent and developed by slow evaporation technique. The XRD crystal data is obtained and compared with the experimental data by which a good agreement is achieved. The FT-IR spectrum of the compound was recorded in the region 4000-400 cm<sup>-1</sup> and simulations were performed with the theoretical data. Normal coordinate analysis was carried out to the compound using DFT force field revised by a recommended set of scaling factors producing fairly good agreement between the observed and computed frequencies. The total electron density in the molecule and three dimensional molecular electrostatic potential maps of the titled molecule was built by using B3LYP/6-311++G\*\* basis set to visualize electrostatic potential (e<sup>-</sup> + nuclei) distribution, nucleophilic and electrophilic substitution within the molecule. HOMO, LUMO orbitals along with their energies were calculated and explained. Stability of the titled compound originating from hyper conjugative interactions and charge transfer within the molecule has been examined by applying natural bond orbital (NBO) analysis. Dipole moment (D), polarizability (α), hyperpolarizability (β), global softness, energy gap (ΔE), Ionization Potential (I), chemical potential (μ) were calculated to examine the NLO application of our title compound. The Fluorescence spectra at different excitation wavelengths were recorded, analysed and presented.*

**Keywords:** Benzothiophenesulfone-2-methanol (BS2M), FT-IR, XRD, UV-Vis spectra, fluorescence spectra.

## 1. Introduction

Benzothiophene belongs to a branch of heterocyclic compounds consist of a phenyl ring fused with five membered stable aromatic rings made up of sulfur as heteroatom having molecular formula C<sub>8</sub>H<sub>6</sub>S and smell equivalent to naphthalene. It appears commonly as a combining of petroleum-analogue deposits like lignite tar. Benzothiophene molecule has no domestic use. It was used mainly in pharmacy industry and research and development. Based on the nature of heterocyclic compound, benzothiophene assumes to use in research as a starting material for the synthesis of bigger, generally bioactive type structure. It was occurred mainly in the form of pharmaceutical drug products namely such as raloxifene, Zieuton, and Sertaconazole, and also BTCP. Benzothiophene was also used as a material for synthesis of dyes namely Thioindigo. As benzothiophene is aromatic compound, it shows large stability and also has reactive sites within the structure which permits to functionalization. Thiophene similar derivatives are a very impressive type of compounds with various utilities in industrial and medicinal chemistry. Benzothiophene type Skelton structures were usually occurred in electronic components also in biologically active compounds. The Benzothiophene structure was occurred in medicinally active compounds namely raloxifene (selective estrogen receptor

UGC JOURNAL NO. 45204;

[https://www.ugc.ac.in/journallist/ugc\\_admin\\_journal\\_report.aspx?eid=NDUyMDQ=](https://www.ugc.ac.in/journallist/ugc_admin_journal_report.aspx?eid=NDUyMDQ=)  
IMPACT FACTOR: 4.977 Page | 5



modulators), arzoifene (ant tubulin agents) and Zileuton (selective inhibitor of 5-lipoxygenase). Therefore, the improvement of helpful synthetic procedures to these-sulfur-containing heterocycles has collected adequate consideration during the past decades. Nevertheless distinguished with another heteroaromatic rings, especially its analogues Benzofuran, Indole and Benzothiophene skeleton are rather limited. The best accepted approach was based on the intra-molecular cyclization procedures.

Vibrational spectroscopy is the greatest and extensively used approach in spectroscopy and this method is useful to study the structural properties of most of the organic compounds. The theoretical computations and experimental investigations on vibrational spectra of benzothiophene and its derivatives were reported in literature time to time. Measurement of the complete set of vibrational wavenumbers for Benzothiophene in the gas state was undertaken using Fourier-transform FT-IR and Raman Spectroscopy. Additionally, several types of condensed-phase spectra were observed. Indene and their heterocyclic derivatives have broad biomedical and industrial uses of that benzothiophene and benzothiazole are sulfur-consisting derivatives. Benzothiazoline-2-thione compound was suitable for bonding with metal ions broadly used as extensive rubber vulcanization accelerator (Ellis et al. 1966), corrosion inhibitor and impressive platform of minerals. The heterocyclic compounds consisting of a thiazole ring have been used as fungicides, herbicides and plant development regulators. Given assert to Thiazole derivatives, because their biological importance was found in the penicillin which is a derivative of Thiazole ring and used as a therapeutic agent. The compound was collected over organocatalyzed reactions starting from 3-substituted halobenzothiophenecarbaldehydes. Anti-bromobenzothiophene type structures show strong halogen... $\pi$  interactions between Bromine and the Heterocyclic phenyl ring, corresponding to energy of  $7.5\text{kcalmol}^{-1}$ . Syn-Bromo and Syn-Iodo substituted compounds appeared to be similar structure, Showing X...O (Carbonyl) interactions,  $\pi$  stacking, and formation of extended hydrogen bonding networks (Cadoni et al. 2014). In diesel and gas oils the amount of sulfur not less than 30 ppm because, it was the main target in the refining industry. So these impurities were necessary for heterocyclic compounds like benzothiophene (BT) and dibenzothiophene (DBT).

However, in literature, there was no research work done on the quantum chemical studies of Benzothiophene sulfone-2-methanol. Therefore, in the present study, we report the XRD, vibrational, UV, Fluorescence spectra studies on Benzothiophene sulfone-2-methanol using DFT calculations for the first time.

## 2. Experimental Details

The powder sample of Benzothiophene sulfone-2-methanol was obtained from sigma Aldrich chemical company (USA) with a stated purity of 97% and it was used as such for spectral measurements without further purification.

### 2.1 FT-IR Spectrum

Fourier transform Infrared spectrum of the compound is measured at  $302.15^\circ\text{K}$  temperature in the region  $4000\text{-}400\text{cm}^{-1}$  using Nicolet 6700 FT-IR spectrometer assembled with a Thermo Nicolet Continuous IR microscope or high performance single bound diamond attenuated total reflectance (ATR) accessory and by a Reni Shaw in via., Raman microscope with UV or visible laser excitation at a resolution of  $4\text{cm}^{-1}$ .

### 2.2 UV-Vis and Fluorescence spectrum

Electronic spectrum of the examined compound was measured in the range of 300-1100 nm utilizing a Perkin Elmer Lambda 35 UV-Vis spectrometer. Experimental data was recorded after 1 cycle, with an



interval of 1 nm, slit width of 2 nm and scan speed of  $240 \text{ nm}\cdot\text{min}^{-1}$  with the spectral resolution of 0.05-4.0 nm. Fluorescence and UV-Vis spectrum were recorded using methanol as solvent. The slit width was set to 15 nm for the excitation monochromator and to 10 nm for the emission monochromator.

### 3. Computational Details

All the theoretical computations in this paper were performed with the help of Gaussian 09W program (Frisch et al. 2009) Gauss-View 5.0 molecular visualization program package (Dennington et al. 2016) on personal computer. The most optimized structure which was obtained by PES analysis and its molecular properties, energy and vibrational wave numbers in  $\text{cm}^{-1}$  of the investigated compound were calculated by using B3 (Becke et al. 1988) mutual change functional using with the LYP (Lee et al. 1988) correlation functional resulting in the B3LYP density functional method at 6-311++G\*\* basis set. This method was broadly approved for calculating vibrational wave numbers of biologically active organic structures. Mostly, the computed vibrational wave numbers were larger than the experimentally recorded wave numbers because of an-harmonic effect, electron correlation effects and the deficiency in the basis set. So, to develop the coincidence between the computed and observed frequencies, the computed harmonic frequencies were scaled down for comparison. For this purpose, we used a scaled quantum mechanical (SQM) procedure to the examined compound. The vibrational assignments together with their potential energy distribution (PED) were performed with the MOLVIB (version 7) program developed by T. Sundius (Sundius et al. 1991). NBO analysis was worked out using NBO program available in the Gaussian 09W package at DFT/B3LYP/6-311++G\*\* level of theory in order to understand the intra-molecular delocalization, charge transfer within the molecule, stabilization energy of the molecule. UV-Vis spectrum is predicted using TD DFT calculations supplementing with 6-311++G\*\* basis set.

### 4. Results and Discussion

#### 4.1. X-ray crystallographic studies

Single crystal X-ray diffraction measurements of the title compound were carried out on Bruker axk kappa apex2 CCD Diffractometer with Mo Ka radiation (0.71073) at  $296^\circ \text{K}$  (Table 1). Data reduction was performed with the SAINT program and the structure was solved using the SIR92 program. SHELXL97 program was used for the refinement of the structure. Structure-invariant direct methods were used for primary atom site locations and secondary atom site locations were found from the difference Fourier map. The positions of all aromatic and aliphatic CAH hydrogen atoms were calculated geometrically and a riding model was used in the refinement, with C-H distances in the range of 0.93–0.98 Å and  $U_{\text{iso}}(\text{H}) = 1.2U_{\text{eq}}(\text{C})$ . All the N-H and O-H hydrogens were refined from difference Fourier maps. The software used to prepare the material for publication was Mercury 2.3 (Build RC4) and ORTEP- 3. The ORTEP and packing diagrams of the title compound are presented in Figure 1 and Figure 2 respectively. The complete set of structural parameters of molecule in the CIF format was already submitted and is available from the Cambridge Crystallographic Database Center under CCDC No.1505584.

Table-1: Crystallographic data for the title compound

Empirical formula	C <sub>9</sub> H <sub>8</sub> O <sub>3</sub> S
Formula weight	196.21
Temperature	296°K
Wavelength	0.71073 Å

UGC JOURNAL NO. 45204;

[https://www.ugc.ac.in/journallist/ugc\\_admin\\_journal\\_report.aspx?eid=NDUyMDQ=](https://www.ugc.ac.in/journallist/ugc_admin_journal_report.aspx?eid=NDUyMDQ=)

IMPACT FACTOR: 4.977 Page | 7

Crystal system	Monoclinic P21/c
Unit cell dimensions	a = 9.551(4) Å b = 10.973(5) Å c = 16.569(8) Å $\alpha = 90^\circ$ $\beta = 97.297^\circ$ (2) $\gamma = 90^\circ$
Volume	1722.65(14) Å <sup>3</sup>
Z	8
Absorption coefficient	0.343 mm <sup>-1</sup>
F(000)	816
Crystal size	0.35 x 0.30 x 0.30 mm
Theta range for data collection	2.23 to 28.35 deg.
Limiting indices	-14 ≤ k ≤ 14 -22 ≤ l ≤ 21 -12 ≤ h ≤ 12
Reflections collected / unique	18617 / 4152 [R(int) = 0.0174]
Max. and min. transmission	0.9042 and 0.8895
Data / restraints / parameters	4152 / 0 / 242
Goodness-of-fit on F <sup>2</sup>	1.009
Final R indices [I > 2σ(I)]	R1 = 0.0330, wR2 = 0.0948
R indices (all data)	R1 = 0.0393, wR2 = 0.1015

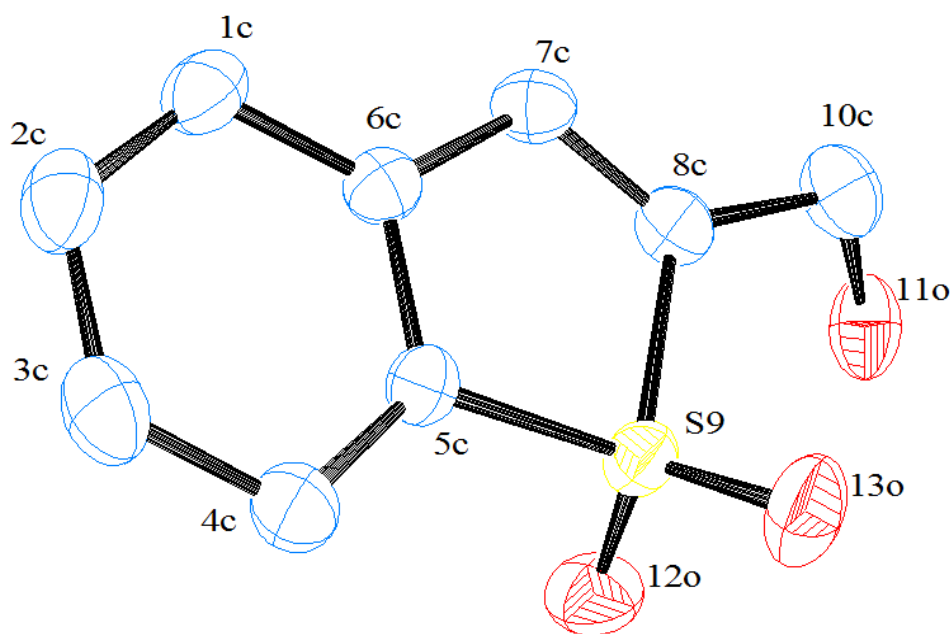


Figure-1: ORTEP diagram of the molecule drawn at 50% probability.

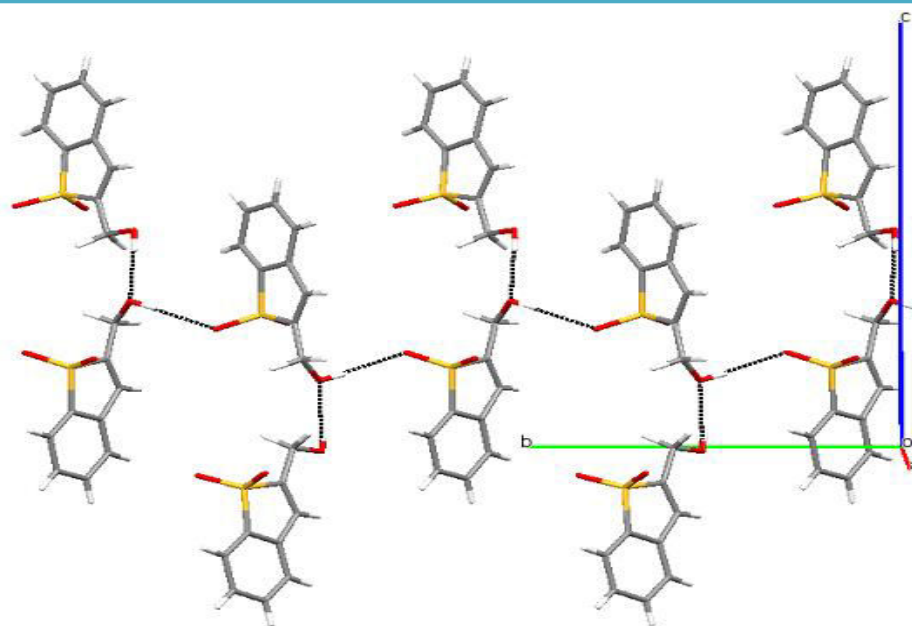


Figure-2: The packing diagram of the molecule viewed along 'b' axis.

#### 4.2. Molecular Structure

Initially, from the ground state optimized structural parameters of the examined compound i.e. bond lengths, bond angles were calculated by DFT/B3LYP/6-311++G\*\* level of theory were tabulated in Table 2 according to the numbering scheme obtained from Gauss view as represented in Fig.3. These structural parameters are now estimated with the exact experimentally measured X-ray data of Benzothiophenesulfone-2-methanol. According to the data seen in Table 2, it was observed that the few bond lengths are found to be higher than experimental values. These deviations are obvious since the computations belong to isolated molecule in gas phase and the experimental values belong to the exact molecule in solid state. In order to reveal all possible conformations of BS2M, The potential energy surface (PES) scan for C7-C8-C10-O11 was observed by changing the torsion angle for every 10° un to 360° rotation all over the bond using B3LYP/6-311++G\*\* basis set. The plot between the potential energy as a scan of the torsional angle is presented in Fig.4. The minimum energy at dihedral angle 0° (stable conformer) obtained from potential energy vs. dihedral angle plot was -971.5350476 Hartrees. Further, it was observed that the large deviation between the computed and experimental for bond lengths was 0.036Å for C5-S9. In case of bond angles, it was 4.78Å for C8-C10-O11. The benzene ring in the molecule BS2M appears to be a small distortion which is proven for CCC bond angle differences. In Thiophene ring of BS2M, the calculated bond lengths of C5-C6, C6-C7 atoms were 1.402 Å, 1.473Å and these values were very close to experimental values, viz., 1.393 Å and 1.472Å respectively. In spite of the fact that the computed results are not exactly coincidence to the observed values of this compound, they are generally accepted that the bond lengths, bond angles depend on the various methods and the basis sets that are used in the quantum chemical calculations, and they can be utilized as base to measure the molecular parameters for the compounds.

Table-2: Optimized geometrical parameters of Benzothiophene sulfone-2-methanol obtained by B3LYP/6-311++G\*\* density functional calculations.

	Value(Å)			Value( °)	
Bond length(A <sup>0</sup> ) <sup>a</sup>	6-311++G**	Exp	Bond angle (A <sup>0</sup> ) <sup>a</sup>	6-311++G**	Exp



C1-C2	1.399	1.391	C1-C2-C3	121.05	121.37
C2-C3	1.396	1.381	C2-C3-C4	120.38	120.79
C3-C4	1.402	1.397	C3-C4-C5	117.60	116.64
C4-C5	1.382	1.371	C4-C5-C6	123.13	123.82
C5-C6	1.402	1.393	C5-C6-C1	118.66	118.68
C6-C7	1.473	1.472	C6-C1-C2	119.15	118.67
C7-C8	1.339	1.330	C5-C6-C7	113.31	112.86
C8-S9	1.807	1.772	C6-C7-C8	115.02	115.01
C5-S9	1.799	1.763	C7-C8-S9	110.48	109.74
C8-C10	1.491	1.493	C10-C8-S9	119.20	119.91
C10-O11	1.416	1.410	C6-C5-S9	109.13	108.71
O12-S9	1.472	1.438	C4-C5-S9	127.72	127.44
O13-S9	1.472	1.441	C7-C8-C10	130.30	130.20
C1-H14	1.086	-	C1-C6-C7	128.01	128.46
C2-H15	1.085	-	C8-C10-O11	108.36	113.14
C3-H16	1.085	-	O12-S9-O13	119.03	116.88
C4-H17	1.085	-	O12-S9-C5	111.21	112.11
C7-H18	1.084	-	O13-S9-C5	111.21	110.38
C10-H19	1.102	-	O12-S9-C8	110.03	110.08
C10-H20	1.102	-	O13-S9-C8	110.02	111.46
			C5-S9-C8	92.03	93.54

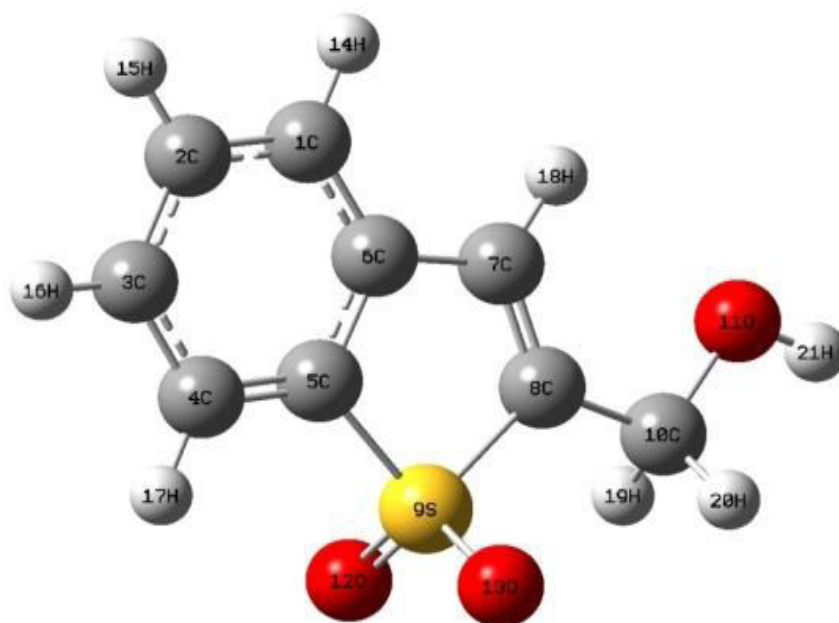


Figure-3: Optimized structure of Benzothiophene sulfone-2-methanol along with numbering of atom.



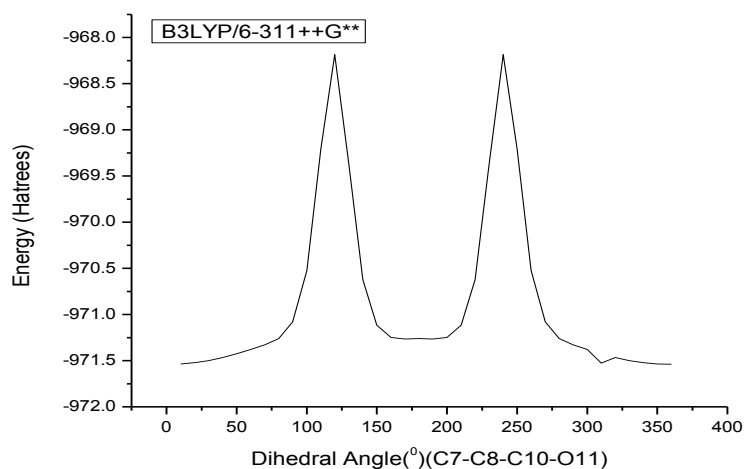


Figure-4: Potential energy surface scan for dihedral angle C7-C8-C10-O11 of Benzothiophene sulfone-2-methanol

### 4.3. Vibrational analysis

First of all vibrational spectral assignments has been performed on BS2M with the help of recorded FT-IR spectrum and theoretically predicted wavenumbers. The title compound is Raman inactive since it is highly fluorescent material. BS2M has to  $C_1$  point group symmetry. As it has  $C_1$  point group symmetry, a compound which consists of N atoms,  $3N-6$  number of vibrational modes are possible apart from three translation motion and three rotational degrees of freedom. Hence, BS2M molecule has 21 atoms with 57 normal modes of vibrations which span the irreducible representations:

$$73N-6 = 39A' \text{ (in - plane)} + 18A'' \text{ (out - of - plane)}. \quad (1)$$

All 57 fundamental vibrations are active in FTIR spectrum. In order to know the complete assignments of fundamental vibrational frequencies, we used normal coordinate analysis (NCA). A set of non-redundant were defined by suitable linear merging of internal coordinates according to the suggestions of Fogarasi and co-workers were reported in Table 3.

Table-3: Definition of local-symmetry coordinates and the values of corresponding scale factors used to correct the B3LYP/6-311++G\*\* (refined) force field of Benzothiophene sulfone-2-methanol.

No.(i)	Symbol <sup>a</sup>	Definition <sup>b</sup>	Scale factors
Stretching			
1 -5	$\nu(\text{C-H})$	R1, R2, R3, R4, R5	0.910
6-13	$\nu(\text{C-C})_{\text{ar}}$	R6,R7,R8,R9,R10,R11,R12,R13	0.900
14	$\nu(\text{C-C})_{\text{sub}}$	R14	0.900
15-16	$\nu(\text{C-S})$	R15,R16	0.980
17	$\nu(\text{S-O})_{\text{SS}}$	$(R17+R18)/\sqrt{2}$	0.910
18	$\nu(\text{S-O})_{\text{AS}}$	$(R17-R18)/\sqrt{2}$	0.910
19	$\nu(\text{C-O})$	R19	0.910
20	$\nu(\text{C-H})_{\text{SS}}$	$(R20+R21)/\sqrt{2}$	0.910



21	$\nu(\text{C-H})_{\text{AS}}$	$(R_{20}-R_{21})/\sqrt{2}$	0.910
22	$\nu(\text{OH})_{\text{Sub}}$	R22	0.810
In-Plane bending			
23-27	$\beta_{\text{C-H}}$	$(\gamma_{23}-\gamma_{24})/\sqrt{2}, (\gamma_{25}-\gamma_{26})/\sqrt{2}, (\gamma_{27}-\gamma_{28})/\sqrt{2}, (\gamma_{29}-\gamma_{30})/\sqrt{2}, (\gamma_{31}-\gamma_{32})/\sqrt{2}$	0.800
28	$\beta_{\text{R1tri}}$	$(\gamma_{33}-\gamma_{34}+\gamma_{35}-\gamma_{36}+\gamma_{37}-\gamma_{38})/\sqrt{6}$	0.910
29	$\beta_{\text{R1asy}}$	$(2\gamma_{33}-\gamma_{34}-\gamma_{35}+2\gamma_{36}-\gamma_{37}-\gamma_{38})/\sqrt{12}$	0.910
30	$\beta_{\text{R2asy}}$	$(a-b)(\gamma_{40}-\gamma_{43})+(a+b)(\gamma_{41}-\gamma_{42})$	0.910
31	$\beta_{\text{R1sym}}$	$(\gamma_{34}-\gamma_{35}+\gamma_{37}-\gamma_{38})/2$	0.910
32	$\beta_{\text{R2sym}}$	$\gamma_{39}+a(\gamma_{40}+\gamma_{43})-b(\gamma_{41}+\gamma_{42})$	0.910
33	$\beta_{\text{C-C-C sub}}$	$(\gamma_{44}-\gamma_{45})\sqrt{2}$	0.930
34	$\beta_{\text{So2 sc}}$	$(\gamma_{46}+\gamma_{48}+\gamma_{47}+\gamma_{49})/2$	0.950
35	$\beta_{\text{So2 ro}}$	$(\gamma_{46}+\gamma_{48}-\gamma_{47}-\gamma_{49})/2$	0.950
36	$\beta_{\text{So2 wa}}$	$(\gamma_{46}-\gamma_{48}+\gamma_{47}-\gamma_{49})/2$	0.950
37	$\beta_{\text{So2 tw}}$	$(\gamma_{46}-\gamma_{48}-\gamma_{47}+\gamma_{49})/2$	0.950
38	$\beta_{\text{C-C-O sub}}$	$\gamma_{50}$	0.930
39	$\beta_{\text{C-O-H sub}}$	$\gamma_{51}$	0.940
40	$\beta_{\text{CH2 sc}}$	$(\gamma_{52}+\gamma_{54}+\gamma_{53}+\gamma_{55})/2$	0.930
41	$\beta_{\text{CH2 ro}}$	$(\gamma_{52}+\gamma_{54}-\gamma_{53}-\gamma_{55})/2$	0.930
42	$\beta_{\text{CH2 wa}}$	$(\gamma_{52}-\gamma_{54}+\gamma_{53}-\gamma_{55})/2$	0.930
43	$\beta_{\text{CH2 tw}}$	$(\gamma_{52}-\gamma_{54}-\gamma_{53}+\gamma_{55})/2$	0.930
Out of plane bending			
44-48	$\omega_{\text{C-H}}$	$\rho_{56}, \rho_{57}, \rho_{58}, \rho_{59}, \rho_{60}$	0.970
49	$\omega_{\text{C-C sub}}$	$\rho_{61}$	0.970
Torsions			
50	$\tau_{\text{R1tri}}$	$(\tau_{62}-\tau_{63}+\tau_{64}-\tau_{65}+\tau_{66}-\tau_{67})/\sqrt{6}$	0.960
51	$\tau_{\text{R1asy}}$	$(\tau_{62}-\tau_{64}+\tau_{65}-\tau_{67})/2$	0.960
52	$\tau_{\text{R2asy}}$	$b(\tau_{69}+\tau_{71})+a(\tau_{68}+\tau_{69})+\tau_{70}$	0.960
53	$\tau_{\text{R1sym}}$	$(-\tau_{62}-2\tau_{63}-\tau_{64}+\tau_{65}+2\tau_{66}-\tau_{67})\sqrt{12}$	0.960
54	$\tau_{\text{R2sym}}$	$(a-b)(\tau_{71}-\tau_{69})+(1-a)(\tau_{72}-\tau_{68})$	0.960
55	Butter	$(\tau_{73}-\tau_{74})/2$	0.990
56	$\tau_{\text{SCCO}}$	$(\tau_{75}+\tau_{76})/2$	0.990
57	$\tau_{\text{CCOH}}$	$\tau_{77}$	0.990

Where  $a=\cos 144^\circ$ ,  $b=\cos 72^\circ$ .

Abbreviations:  $\nu$ , stretching;  $\beta$ , in plane bending;  $\omega$ , out of plane bending;  $\tau$ , torsion, ss, symmetrical stretching, ass, asymmetrical stretching, sc, scissoring, wa, wagging, tw, twisting, ro, rocking, tri, trigonal deformation, sym, symmetrical deformation, asy, asymmetric deformation, butter, butterfly, ar, aromatic, sub, substitution.

<sup>a</sup> These symbols are used for description of the normal modes by PED in Table 3.

<sup>b</sup> The internal coordinates used here are defined in table given in supplementary material 1

The elaborated fundamental vibrational assignments of BS2M along with the measured IR intensities and normal mode interpretations represented by potential energy distribution are tabulated in Table 4. By using suitable scaling, the visual similarity of simulated IR spectra has represented in Fig.5,

UGC JOURNAL NO. 45204;

[https://www.ugc.ac.in/journallist/ugc\\_admin\\_journal\\_report.aspx?eid=NDUyMDQ=](https://www.ugc.ac.in/journallist/ugc_admin_journal_report.aspx?eid=NDUyMDQ=)

IMPACT FACTOR: 4.977 Page | 12





respectively. The below expression was used to measure the root mean square (RMS) values of frequencies.

$$RMS\ Error = \sqrt{\frac{1}{n-1} \sum_i^n (v_i^{calc.} - v_i^{exp.})^2} \quad (2)$$

The RMS variation of the theoretical and measured frequencies was found to be 79.01. Thereafter, to reduce this variation between the observed and scaled quantum mechanical (SQM) vibrational frequencies, different scale factors were used reduce it to a deviation of 5.8. This shows that the theoretical IR spectrum of the titled compound agrees well with the recorded FT-IR spectrum. For the complete understanding, we have shown the experimental and simulated FT-IR spectra of BS2M in Fig. 5.

Table-4: Detailed assignments of fundamental vibrations of Benzothiophene sulfone-2-methanol by normal mode analysis based on SQM force field calculations using B3LYP/6-311++G\*\*]

S.No	Experimental (cm <sup>-1</sup> ) FT-IR	Symmetry species	Scaled frequencies (cm <sup>-1</sup> )	Un-scaled frequencies (cm <sup>-1</sup> )	Intensity I <sub>IR</sub> <sup>b</sup>	Characterization of normal modes with PED (%) <sup>c</sup>
1	3450vs	A	3452	3835	21.04	vOH(100)
2		A	3082	3228	0.89	vCH(99)
3		A	3072	3217	6.87	vCH( 99)
4	3060ms	A	3063	3208	5.54	vCH(99)
5		A	3055	3199	3.96	vCH( 99)
6		A	3045	3188	0.96	vCH(99)
7	2930w	A	2921	3001	14.25	vCHas(99)
8	2870w	A	2848	2977	14.21	vCHss(100)
9	1660vw	A	1621	1702	0.27	vCCar(71), βCH2sc(12),
10	1580s	A	1571	1649	2.23	vCCar(66), βR2sym(12), βR1sym(10),
11		A	1556	1633	7.12	βCH2sc (53), vCCar( 30)
12		A	1546	1523	0.44	vCCar(61), βCH2sc (15)
13	1450s	A	1485	1501	15.86	βCH2wa(76), vCCsub (10)
14		A	1383	1490	6.00	vCCar (60), βCCC (33)
15		A	1370	1463	2.78	vCCar (52), βCH(38)
16	1300s	A	1308	1381	0.53	vCCar (79), βR2sym(10)
17		A''	1287	1321	0.43	βCH2tw(98)
18		A	1232	1296	26.35	vCCsub(36), βOHsub( 25), βCH(18)
19		A	1181	1284	15.95	βOHsub(36), βCH (27), vCCar(21),
20		A	1171	1251	1.13	βCH (49), vCCar(17), βR2asy(10)
21	1140w	A	1125	1233	3.43	βCH( 26), vCS(22), vCCar(15), vCCsub(10)
22	1100w	A	1091	1202	100	vSOas( 89)
23		A	1079	1189	15.29	βRtri(26), βCH(24), vCCar(24), vCS(19)
24		A''	1069	1156	0.92	βCH2ro(82)
25		A	1058	1131	2.53	βCH (83), vCCar(13)



26		A	1043	1115	10.46	vCO (54) $\beta$ Rtri( 20), vCCsub(13), vCCar (10)
27		A	1028	1064	11.82	$\beta$ CH (42), vCCar(23), vCCsub(19)
28		A	976	1052	3.33	vCCar(64), $\beta$ CH(33)
29		A	968	1045	0.07	$\omega$ CH (88), $\tau$ R1tri (10)
30		A''	942	1041	85.76	vSOss (73)
31		A''	925	995	1.29	$\omega$ CH (90), $\tau$ Rlasy(7)
32	896s	A''	886	952	7.95	$\omega$ CH( 80), $\tau$ R2asy(9), $\tau$ R1tri (6)
33		A''	851	906	2.48	$\omega$ CH ( 94)
34		A	845	874	1.88	$\beta$ R2asy ( 35), $\beta$ R2sym ( 22), vCCar ( 16), vCCsub ( 14)
35		A	811	867	19.58	$\beta$ CH(42), $\beta$ COsub(14), vCCar(10)
36	780w	A''	751	769	6.92	$\tau$ R1tri (50), $\omega$ CH ( 36)
37		A''	743	740	12.92	$\omega$ CH ( 55), $\tau$ R1tri (35)
38		A	739	736	5.64	vCS( 29), $\beta$ R2sym( 12), $\beta$ Rlasy( 10)
39		A	700	712	10.67	$\beta$ Rlasy(25), vCS( 21), vCCar(14), $\beta$ R1sym(11)
40		A	612	616	5.13	$\beta$ R1sym(39), $\beta$ R2asy(26), vCS (17)
41	577vw	A''	565	564	8.05	$\tau$ R2asy(44), $\omega$ CCsub( 17)
42		A''	563	555	44.85	$\beta$ SO2wa(42), $\beta$ R1asy(10)
43	552vw	A''	549	546	2.30	$\tau$ R1sym(35), $\tau$ R1tri(14), $\tau$ SO2ro(14), $\omega$ CH(13), $\tau$ R2sym(12)
44		A	540	543	17.01	$\beta$ R2sym (32), $\beta$ SO2sc(27), $\beta$ Rlasy(12)
45		A''	450	456	1.49	vCCar(20), vCS (15), $\beta$ R1sym(14), $\beta$ R2asy(11), $\beta$ R2sym(10)
46		A''	432	436	1.32	$\tau$ Rlasy(46), $\tau$ butt (19), $\tau$ R1sym(11)
47		A	374	371	3.05	$\beta$ SO2sc(48), $\beta$ R2sym(39)
48		A''	323	322	0.67	$\tau$ Rlasy(35), $\beta$ SO2tw(18), $\omega$ CCsub(13), $\omega$ CH (13), $\tau$ R1sym(10)
49		A	314	309	0.80	vCS ( 40), $\beta$ COsub ( 25), $\beta$ CH2sc (10)
50		A''	279	274	0.97	$\tau$ R1sym ( 29), $\tau$ R2asy ( 28), $\beta$ SO2ro ( 22)
51		A''	233	232	4.02	$\tau$ CS (28), $\beta$ SO2wa(24), $\beta$ R2sym(18)
52		A''	207	208	49.67	$\tau$ CCOH ( 85)
53		A''	145	141	16.76	$\omega$ CCsub( 35), $\beta$ SO2tw( 24), $\tau$ CCOH( 12)
54		A	133	133	2.78	$\beta$ CCsub( 59), $\beta$ COsub( 15)
55		A''	111	113	0.02	$\tau$ butt(48), $\tau$ R2sym(19), $\beta$ SO2tw(17)
56		A''	97	96	9.64	$\tau$ R2sym( 38), $\tau$ SCCO (14), $\tau$ R2asy( 13), $\tau$ butt ( 10),
57		A''	60	60	1.75	$\tau$ SCCO( 61) $\omega$ CCsub( 15)

<sup>a</sup> Abbreviations: v, stretching;  $\beta$ , in plane bending;  $\omega$ , out of plane bending;  $\tau$ , torsion, ss, symmetrical stretching, as, asymmetrical stretching, sc, scissoring, wa, wagging, twi, twisting, ro, rocking, ipb, in-plane bending, opb, out-of-plane bending; tri, trigonal deformation, sym, symmetrical deformation, asy, asymmetric deformation, butt, butterfly, ar, aromatic, sub, substitution, vs, very strong; s, strong; ms, medium strong; w, weak; vw, very weak.

<sup>b</sup>Relative IR absorption intensities normalized with highest peak absorption equal to 100.

<sup>c</sup> Only PED contributions  $\geq 10\%$  are listed.

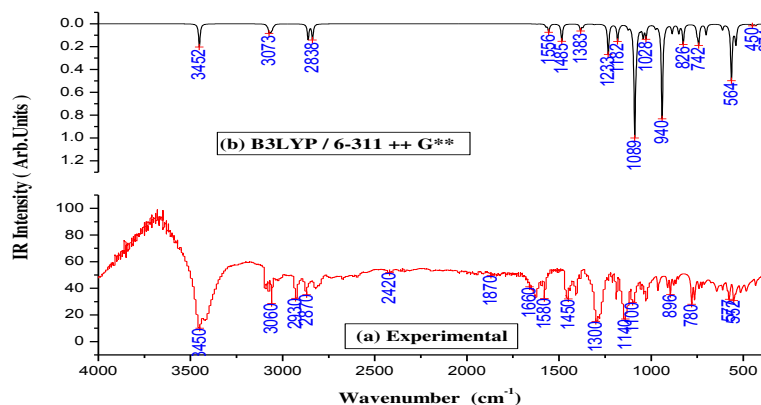


Figure-5: (a) Experimental, (b) Simulated FT-IR spectra of Benzothiophene sulfone-2-methanol.

#### 4.4.1. C-H Vibrations

The fused aromatic and hetero aromatic type of compound shows C-H stretching wave numbers in the range 3100-3000  $\text{cm}^{-1}$  which is the characteristic region for the identification of C-H stretching wavenumbers (Ramalingam et al. 2011). The bands which were not affected significantly in this region. In this region, the molecule has more than three C-H stretching frequencies appeared as umbrella pattern like weak to medium intensity respectively. As it is evident from Table 4, the mode numbers from 2-6 are the C-H stretching vibrational signals scaled at 3082, 3072, 3063, 3055 and 3045  $\text{cm}^{-1}$  and the corresponding C-H vibrations are observed at 3060  $\text{cm}^{-1}$  in the FTIR spectrum. This shows excellent agreement with literature. The aromatic in-plane C-H bending modes of benzene and its derivatives were identified in the region 1350-950  $\text{cm}^{-1}$  and are most probably weak. The calculated frequency 1140  $\text{cm}^{-1}$  is assigned to C-H in-plane bending vibration. The C-H out of plane bending modes normally medium intensity emerges in the region of 950- 600  $\text{cm}^{-1}$ . In the titled compound, the bands observed at 968  $\text{cm}^{-1}$ , 925  $\text{cm}^{-1}$ , 886  $\text{cm}^{-1}$ , 851  $\text{cm}^{-1}$ , and 743  $\text{cm}^{-1}$  are in good agreement with the observed value of 896  $\text{cm}^{-1}$ . The aromatic C-H in-plane and out of plane bending vibrations have considerable overlapping with the ring C-C-C in-plane and out of plane bending modes.

#### 4.4.2. C-C Vibrations

The ring C-C stretching frequency modes generally occur in the region 1650-650  $\text{cm}^{-1}$  (Varsanyi, 1974). Several ring vibrational modes are affected by substitution in the aromatic ring. With heavy substituents, the bands tend to shift somewhat to lower wavenumbers and the greater the number of substituents on the ring the broader the absorption region. In the present study, the scaled frequencies at 1621  $\text{cm}^{-1}$ , 1571  $\text{cm}^{-1}$ , 1546  $\text{cm}^{-1}$ , 1383  $\text{cm}^{-1}$ , 1370  $\text{cm}^{-1}$ , 1308  $\text{cm}^{-1}$ , 1232  $\text{cm}^{-1}$ , and 976  $\text{cm}^{-1}$  are assigned to CC stretching modes, which are mostly mixed with other vibrations. These values show a good agreement with the observed values like 1660  $\text{cm}^{-1}$ , 1580  $\text{cm}^{-1}$  and 1330  $\text{cm}^{-1}$ .

#### 4.4.3. C-O vibrations

The carbonyl stretching frequency has been most extensively studied by infrared spectroscopy. The carbonyl stretching frequency is very sensitive to the factors that disturb the nature of carbonyl group and its precise frequency is characteristic of the type of the carbonyl compound being studied. This region is considered as a very important region by organic chemists. The carbonyl stretching



vibrations in alcohols are expected in the region  $1000-1150\text{ cm}^{-1}$ . In the case of BS2M, the frequency scaled at  $1043\text{ cm}^{-1}$  belongs C-O stretching mode which is not observed in the spectrum.

### **CH<sub>2</sub> vibrations**

The CH<sub>2</sub> group basically contains six fundamental vibrations, such as, CH<sub>2</sub> symmetric stretch; CH<sub>2</sub> asymmetric stretch; CH<sub>2</sub> scissoring and CH<sub>2</sub> rocking, CH<sub>2</sub> wagging and CH<sub>2</sub> twisting. Normally, CH<sub>2</sub> asymmetric and symmetric stretching vibrations occur in the region  $3000 \pm 45\text{ cm}^{-1}$  and  $2950 \pm 45\text{ cm}^{-1}$ . Therefore, the mode scaled at  $2921\text{ cm}^{-1}$  is observed at  $2930\text{ cm}^{-1}$  is assigned to CH asymmetric stretching mode. Similarly, the band observed at  $2870\text{ cm}^{-1}$  is assigned to CH symmetric stretching mode whose counterpart is scaled at  $2838\text{ cm}^{-1}$ . CH<sub>2</sub> scissoring frequency observed at  $1556\text{ cm}^{-1}$ , CH<sub>2</sub> wagging frequency observed at  $1485\text{ cm}^{-1}$ , CH<sub>2</sub> twisting frequency observed at  $1287\text{ cm}^{-1}$  and CH<sub>2</sub> rocking frequency observed at  $1069\text{ cm}^{-1}$  respectively. The recorded FT-IR value occurred at  $1450\text{ cm}^{-1}$ .

### **OH Vibrations**

The O-H stretching vibrations normally occurred in the region  $3500 - 3600\text{ cm}^{-1}$  of infrared spectrum. In the case of BS2M, the value observed at  $3452$  which is a very strong intensity band and good agreement with the recorded FT-IR spectra at  $3450\text{ cm}^{-1}$  which had a maximum PED distribution (100).

### **C-S Vibrations**

The C-S stretching bands are usually observed in the range,  $570-710\text{ cm}^{-1}$  (Arivazhagan et al. 2014) with a moderate intensity. In the case of BS2M the theoretical value observed at  $739\text{ cm}^{-1}$  is assigned to CS stretching mode.

### **SO<sub>2</sub> Vibrations**

Generally, SO<sub>2</sub> symmetric stretching frequency observed in the range  $1250 - 1350\text{ cm}^{-1}$ , asymmetric stretching frequency observed in the region  $1100 - 1300\text{ cm}^{-1}$ . Bending modes are observed in the region of  $350 - 500\text{ cm}^{-1}$ . In the titled compound, the symmetric stretching mode was observed at  $942\text{ cm}^{-1}$ , asymmetric stretching mode was observed at  $1091\text{ cm}^{-1}$ . Asymmetric stretching frequency value was good agreement with the observed FT-IR spectrum and bending modes were also occurred at  $374\text{ cm}^{-1}$ ,  $563\text{ cm}^{-1}$ .

## **5. NBO analysis**

NBO analysis gives information about the most precise possible natural Lewis structure picture of  $\phi$ , because all the orbital characteristics are mathematically selected to contain the most possible percentage of the electron cloud. By the utilization of second-order bond, anti-bond (receptor-donor) NBO energetic analysis, perception in the important delocalization procedures was obtained. The change in the electron cloud in the ( $\sigma^*$ ,  $\pi^*$ ) anti-bonding orbitals and  $E^{(2)}$  energies has been measured by natural bond orbital analysis (NBO) using Density functional theory method to give understandable evidence of stabilization originating from different molecular interactions. Natural bond orbital (NBO) analysis has been performed on the titled compound BS2M, to know the intra-molecular hydrogen bonding, intra-molecular charge transfer (ICT) interactions and delocalization of



$\pi$ -electrons of the fused heterocyclic benzothiophene ring. Further, by using the second order perturbation theory hyper conjugative interaction energy was obtained For each donor (i) and acceptor (j), the stabilization energy  $E^{(2)}$  associated with the delocalization  $i \rightarrow j$  is calculated as

$$E^{(2)} = - n_{\sigma} \frac{\langle \sigma | F | \sigma \rangle^2}{\epsilon_{\sigma^*} - \epsilon_{\sigma}} = - n_{\sigma} \frac{F_{ij}^2}{\Delta E} \quad (3)$$

Where,  $\langle \sigma | F | \sigma \rangle^2$  or  $F_{ij}^2$  is the Fock matrix element i and j NBO orbitals,  $\epsilon_{\sigma^*}$  and  $\epsilon_{\sigma}$  are the energies of  $\sigma$  and  $\sigma^*$  NBOs and  $n_{\sigma}$  is the population of the donor  $\sigma$  orbital. The larger is the  $E^{(2)}$  value, the more intensive is the interaction between electron donors and electron acceptors, i.e. the more donating tendency from electron donors to electron acceptors and the greater the extent of conjugation of the whole system. Delocalization of electrons takes place from occupied Lewis type bond or lone pair (NBO orbitals) to the unoccupied (antibonding and Rydberg) non-Lewis type NBO orbitals equates to a stabilizing donor-acceptor interaction. The NBO analysis have been performed on the compound under investigation using NBO 3.1 program as developed in the Gaussian 09W program package at the DFT/B3LYP/6-311++G\*\* level. The important interactions in the heterocyclic Thiophene molecule having lone pair O13(3) with that of anti-bonding S9-O13, results a stabilization energy of 22.24 kJ/mol. The interaction between C8-C10 with anti-bonding O11-H21 resulting stabilization energy was 1.78kJ/mol. This denotes very small delocalization. The interaction between C1-C6 with antibonding C2-C3, C4-C5 and C7-C8 resulting stabilization energy 20.23, 19.28 and 12.56 kJ/mole which denotes larger delocalization shown in Table 5.

Table-5: Second order perturbation theory analysis of fock matrix in NBO basis for Benzothiophene sulfone-2-methanol

Donor(i)	Type	Ed/e	Acceptor(j)	Type	Ed/e	E(2)	E(i)-E(j)	f(I,j)
C1-C2	$\sigma$	1.97982	C1-C6	$\sigma^*$	0.02991	2.93	1.27	0.055
	$\sigma$		C6-C7	$\sigma^*$	0.02452	4.40	1.17	0.064
C1-C6	$\sigma$	1.97358	C1-C2	$\pi^*$	0.01376	2.32	1.27	0.049
	$\sigma$		C5-C6	$\pi^*$	0.02834	4.53	1.26	0.067
	$\sigma$		C6-C7	$\sigma^*$	0.02452	2.87	1.18	0.052
C1-C6	$\pi$	1.63743	C2-C3	$\pi^*$	0.21383	20.23	0.28	0.069
	$\pi$		C4-C5	$\pi^*$	0.34674	19.28	0.28	0.066
	$\pi$		C7-C8	$\pi^*$	0.12577	12.56	0.29	0.057
C1-H14	$\sigma$	1.98145	C2-C3	$\sigma^*$	0.01490	3.47	1.10	0.055
	$\sigma$		C5-C6	$\sigma^*$	0.02834	4.43	1.08	0.062
C2-C3	$\sigma$	1.98173	C1-C2	$\pi^*$	0.01376	2.39	1.27	0.049
C2-C3	$\pi$	1.65923	C1-C6	$\pi^*$	0.35305	19.06	0.28	0.066
	$\pi$		C4-C5	$\pi^*$	0.34674	21.92	0.28	0.069
C2-H15	$\sigma$	1.98215	C1-C6	$\sigma^*$	0.02291	3.74	1.10	0.057
	$\sigma$		C3-C4	$\pi^*$	0.01459	3.78	1.09	0.057
C3-C4	$\pi$	1.97567	C4-C5	$\sigma^*$	0.01999	3.29	1.28	0.058
	$\pi$		C5-S9	$\sigma^*$	0.21257	5.11	0.86	0.062
C3-H16	$\sigma$	1.98189	C1-C2	$\pi^*$	0.01376	3.74	1.09	0.057
	$\sigma$		C4-C5	$\sigma^*$	0.01999	3.56	1.11	0.056
C4-C5	$\pi$	1.97847	C3-C4	$\pi^*$	0.01459	2.25	1.29	0.048
	$\pi$		C5-C6	$\pi^*$	0.02834	5.16	1.28	0.073



C4-C5	$\sigma$	1.70097	C1-C6	$\pi^*$	0.35305	20.35	0.30	0.070
	$\sigma$		C2-C3	$\pi^*$	0.31283	16.80	0.30	0.063
	$\sigma$		S9-O12	$\sigma^*$	0.15043	3.05	0.55	0.038
	$\sigma$		S9-O13	$\sigma^*$	0.15045	3.05	0.55	0.038
C4-H17	$\sigma$	1.98138	C2-C3	$\sigma^*$	0.01490	3.28	1.10	0.054
	$\sigma$		C5-C6	$\pi^*$	0.02834	4.37	1.08	0.061
C5-C6	$\pi$	1.96817	C1-C6	$\sigma^*$	0.02291	3.74	1.29	0.062
	$\pi$		C4-C5	$\sigma^*$	0.01999	4.65	1.29	0.069
C5-S9	$\sigma$	1.96598	C1-C6	$\sigma^*$	0.02291	3.67	1.25	0.060
	$\sigma$		S9-O12	$\sigma^*$	0.15043	3.23	0.95	0.051
C6-C7	$\sigma$	1.97109	S9-O13	$\sigma^*$	0.15045	3.23	0.95	0.051
	$\sigma$		C1-C6	$\sigma^*$	0.02291	2.67	1.23	0.051
	$\sigma$		C4-C5	$\sigma^*$	0.01999	2.97	1.24	0.054
	$\sigma$		C8-C10	$\sigma^*$	0.02640	5.12	1.07	0.066
	$\pi$		C1-C6	$\sigma^*$	0.02291	3.08	1.34	0.057
	$\pi$		C8-C10	$\sigma^*$	0.02640	3.21	1.18	0.055
C7-C8	$\pi$	1.90331	C1-C6	$\pi^*$	0.35305	13.07	0.32	0.062
	$\pi$		S9-O12	$\sigma^*$	0.15043	3.44	0.57	0.040
	$\pi$		S9-O13	$\sigma^*$	0.15045	3.44	0.57	0.040
	$\pi$		C10-H20	$\sigma^*$	0.02870	2.32	0.72	0.037
C7-H18	$\sigma$	1.97540	C5-C6	$\pi^*$	0.02834	2.37	1.09	0.045
	$\sigma$		C7-C8	$\pi^*$	0.01660	2.80	1.18	0.051
	$\sigma$		C8-S9	$\sigma^*$	0.21259	5.02	0.69	0.055
C8-S9	$\sigma$	1.96084	C4-C5	$\sigma^*$	0.01999	2.56	1.24	0.051
	$\sigma$		C7-H18	$\sigma^*$	0.01726	4.23	1.13	0.062
	$\sigma$		S9-O12	$\sigma^*$	0.15043	3.06	0.94	0.049
	$\sigma$		S9-O13	$\sigma^*$	0.15045	3.06	0.94	0.049
C8-C10	$\sigma$	1.98159	C6-C7	$\sigma^*$	0.02452	2.18	1.14	0.044
	$\sigma$		C7-C8	$\pi^*$	0.01660	4.37	1.31	0.068
S9-O12	$\sigma$	1.98496	S9-O13	$\sigma^*$	0.15045	2.62	1.23	0.052
S9-O13	$\sigma$	1.98496	S9-O12	$\sigma^*$	0.15043	2.62	1.23	0.052
C10-O11	$\sigma$	1.99347	C8-S9	$\sigma^*$	0.21259	2.72	0.98	0.049
C10-H19	$\sigma$	1.97377	C7-C8	$\pi^*$	0.01660	2.40	1.16	0.047
C10-H20	$\sigma$	1.97378	C7-C8	$\pi^*$	0.12577	3.97	0.55	0.043
C10-H20	$\sigma$	1.97378	C7-C8	$\pi^*$	0.01660	2.40	1.16	0.047
C10-H20	$\sigma$	1.97378	C7-C8	$\sigma^*$	0.12577	3.97	0.55	0.043
O11-H21	$\sigma$	1.98819	C8-C10	$\pi^*$	0.02640	3.15	1.13	0.053
O11	LP	1.96154	C10-H19	$\sigma^*$	0.02870	6.26	0.73	0.061
O11	LP	1.96154	C10-H20	$\sigma^*$	0.02870	6.27	0.73	0.061
O12	LP	1.80364	C5-S9	$\sigma^*$	0.21257	15.78	0.44	0.074
O12	LP	1.80364	C8-S9	$\sigma^*$	1.80364	14.05	0.43	0.070
O12	LP	1.77931	S9-O13	$\sigma^*$	1.77931	22.24	0.55	0.101
O13	LP	1.80348	C5-S9	$\sigma^*$	1.80348	16.02	0.44	0.075
O13	LP	1.80348	C8-S9	$\sigma^*$	1.80348	13.82	0.43	0.069
O13	LP	1.77928	C5-S9	$\sigma^*$	1.77928	4.43	0.43	0.039
O13	LP	1.77928	C8-S9	$\sigma^*$	1.77928	6.41	0.43	0.047
O13	LP	1.77928	S9-O12	$\sigma^*$	1.77928	22.20	0.55	0.101
C4-C5	$\sigma^*$	0.34674	S9-O12	$\sigma^*$	0.15043	2.21	0.26	0.043



## 5. Frontier Molecular Orbitals

To explain various types of reactions and estimating the most reactive position in conjugated molecules, Frontier molecular orbitals (molecular orbitals) are used. The highest occupied molecular orbital (HOMO) and lowest unoccupied molecular orbital (LUMO) are the two different types of molecular orbitals in any type of molecule. The biological activity of the any molecule can be known from the Eigen value of HOMO, LUMO and their energy difference. Molecule having a lowest HOMO-LUMO energy difference which indicates a molecule is highly polarizable with a more chemical reactivity and less kinetic energy stabilization. HOMO which can be considered as the highest excited outer most orbital containing electrons, tend to donate these electrons as an electron donor and hence the ionization potential is directly interconnected to the energy of the HOMO. Second type of molecular orbital LUMO can accept electrons and the LUMO energy is directly interconnected to electron affinity. The important molecular orbitals were investigated for the title compound, HOMO and LUMO, which are represented in Fig. 6. The HOMO is located over the Benzene and Thiophene rings except sulfur atom. The LUMO is located overall the molecule except the atoms C4, H14, H17, O11, H21 respectively. In order to understand the various features of pharmaceutical sciences considering drug design and the Eco toxicological nature of the drug molecules, few new chemical descriptors have been presented. Density functional theory based descriptors have been used in so many ways to understand the structural stability of the molecules and their chemical reactivity by measuring the descriptors like chemical potential, global hardness and electrophilicity index. Using HOMO and LUMO orbital energies, the ionization energy and electron affinity can be represented as:  $I = -E_{\text{HOMO}}$ ,  $A = -E_{\text{LUMO}}$   $\eta = (-E_{\text{HOMO}} + E_{\text{LUMO}})/2$  and  $\mu = (E_{\text{HOMO}} + E_{\text{LUMO}})/2$ . This index calculates the stabilization in energy when the molecule acquired an additional electronic charge from the environment. Electrophilicity has been developed recently to analyze the chemical reactivity of the molecule. It contains information about both electron transfer (chemical potential) and stability (hardness) and is a better descriptor of global chemical reactivity. The chemical hardness and chemical potential is given by the following relations:  $\eta = (I - A)/2$  and  $\mu = -(I + A)/2$ , where I and A are the first ionization potential and electron affinity of the chemical species. For the title compound,  $E_{\text{HOMO}} = -6.63228$  eV,  $E_{\text{LUMO}} = -1.85011$  eV, Energy gap =  $-4.78217$  eV, Electronegativity ( $\chi$ ) =  $8.48239$  eV, Chemical hardness ( $\eta$ ) =  $-2.39108$  eV, chemical potential ( $\mu$ ) =  $-4.24119$  eV, Electrophilicity index ( $\omega$ ) =  $-7.52283$  eV Global Softness ( $\sigma$ ) =  $-0.20911$  eV, respectively and which are shown in Table 6. From the above mentioned values it was shown that the chemical potential of the title compound is negative and it means that the compound is stable. Dipole moment in a molecule is next important electronic property study that produces from non-uniform distribution of charges on the different atoms in a molecule. It is mostly used to understand the intermolecular interactions including the Van der Waal type dipole-dipole attractions, etc., because higher the dipole moment, stronger will be the intermolecular interactions. The calculated dipole moment value for the molecule is  $3.8438$  Debye which indicates that the compound exhibits more molecular interactions. The experimental value of  $\lambda_{\text{max}}$  is  $452.65$  nm.

## 6. Fluorescence Spectrum

The fluorescence spectrum of a titled compound BS2M at different excitation wavelengths 225nm, 235nm and 250 nm was recorded in methanol. For the spectrum recorded at excitation energy 225nm the emission maxima shifts towards longer wavelengths 385 and 503 nm respectively which denotes a bathochromic shift (red shift). For the excitation energy 235nm the maxima shifts to 388 and 475 nm denotes red shift and for 250nm the emission maximum shifts towards 397 nm which also denotes the red shift. The fluorescence spectrum at different wavelengths of the titled compound has been shown in Fig. 9. So from the experimental spectrum, we can conclude that the titled compound BS2M has valid applications including in the laser also.

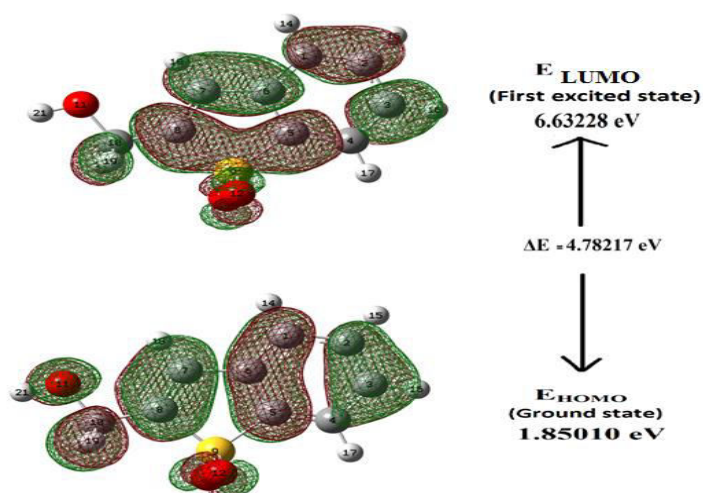


Figure-6: The atomic orbital components of the frontier molecular orbital (HOMO-MO: 51, LUMO-MO: 52) Benzothiophene sulfone-2-methanol

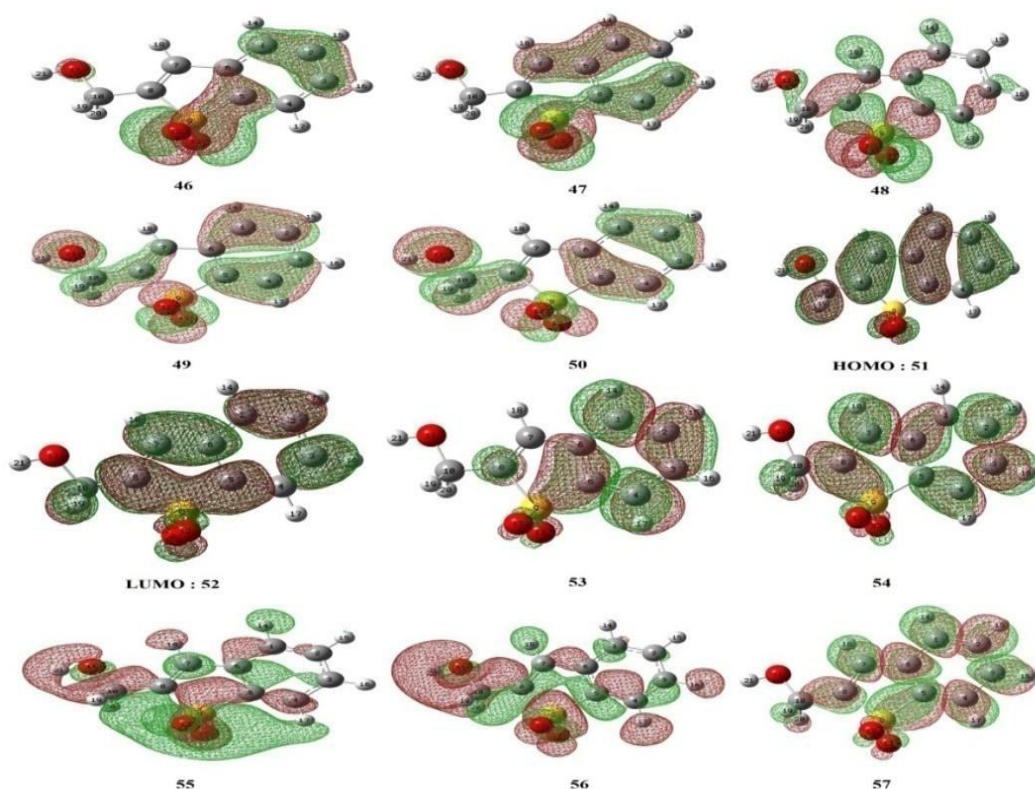


Figure-7: Visualization of the molecular orbitals [MO: 46–MO: 57] of Benzothiophene sulfone-2-methanol under  $C_s$  symmetry: HOMO—MO:51 and LUMO—MO:52.

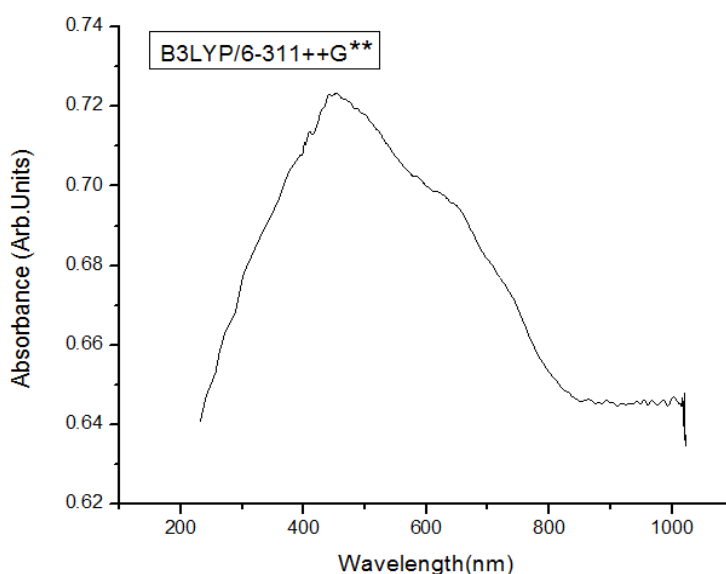


Figure-8: Experimental UV/Vis spectra of Benzothiophene sulfone-2-methanol.

Table-6: The calculated quantum chemical parameters for Benzothiophene sulfone-2-methanol obtained by B3LYP/6-311++G\*\* calculations.

Property	Benzothiophene sulfone-2-methanol
Total energy (eV)	-26437.17
$E_{\text{HOMO}}$ (eV)	-6.63228
$E_{\text{LUMO}}$ (eV)	-1.85010
$E_{\text{HOMO}}-E_{\text{LUMO}}$ (eV)	4.78217
Ionization potential(I) (eV)	-6.63228
Electron Affinity(A) (eV)	-1.85010
Chemical potential ( $\mu$ ) (eV)	-4.24119
Electronegativity ( $\chi$ )eV	4.24119
Chemical hardness( $\eta$ )eV	-2.39108
Electrofilicity index ( $\omega$ ) eV	-3.76141
Global Softness ( $\sigma$ )eV	-0.41822
Total energy change( $\Delta E_{\text{T}}$ ) eV	0.59777
Dipole moment(D)	3.8438

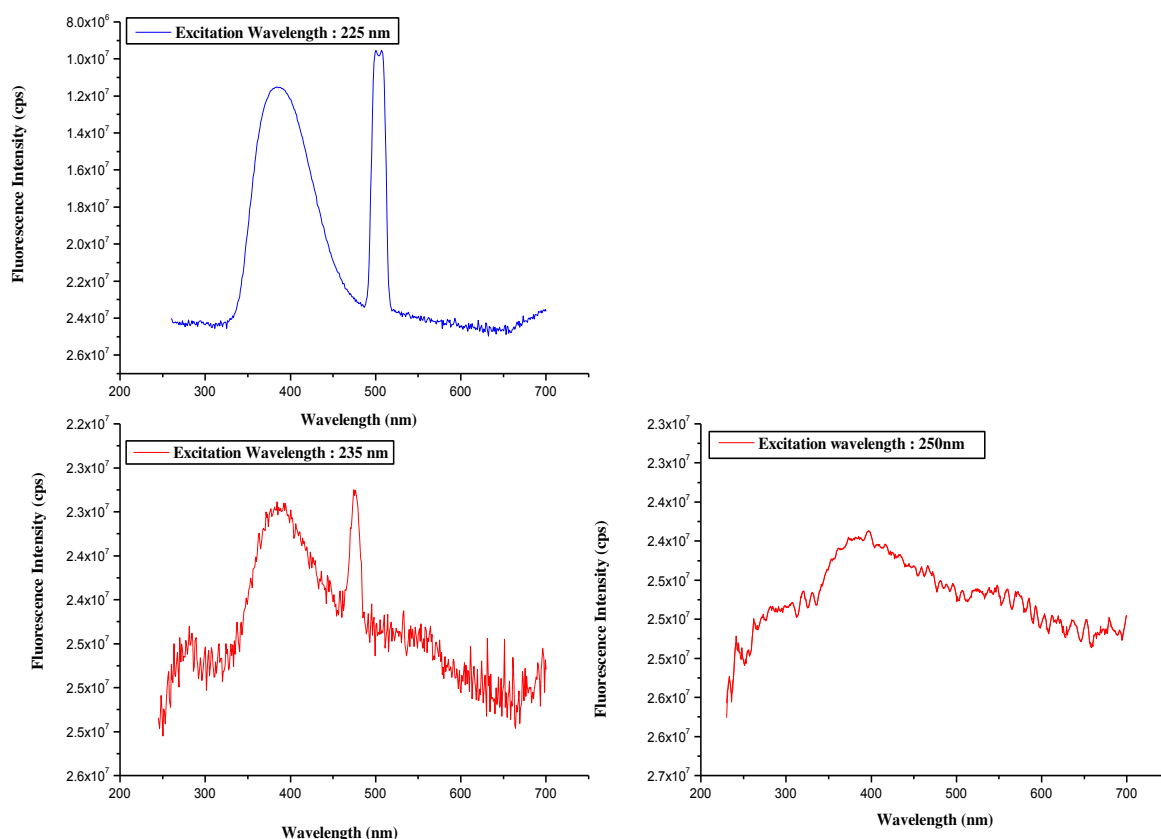


Figure-9: Fluorescence spectra of Benzothiophene sulfone-2-methanol.

## 7. NLO Properties

The second-order polarizability or first hyperpolarizability ( $\beta$ ), dipole moment ( $\mu$ ) and polarizability ( $\alpha$ ) of BS2M was calculated using B3LYP/6-311++G\*\* basis set on the foundation of the finite-field approach. In order to know the results of the DFT/B3LYP methods and calculating the magnitude of total static dipole moment ( $\mu$ ), the mean polarizability ( $\alpha_0$ ), the anisotropy of the polarizability ( $\Delta\alpha$ ) and the mean first hyperpolarizability ( $\beta_0$ ), utilizing the x, y, z elements from Gaussian 09W program package is defined as follows

$$\mu = \mu_x^2 + \mu_y^2 + \mu_z^2 \quad (4)$$

$$\alpha_0 = \frac{\alpha_{xx} + \alpha_{yy} + \alpha_{zz}}{3} \quad (5)$$

$$\Delta\alpha = 2^{-1/2} [(\alpha_{xx} - \alpha_{yy})^2 + (\alpha_{yy} - \alpha_{xx})^2 + 6\alpha_{xx}^2]^{1/2} \quad (6)$$

$$\beta = (\beta_x^2 + \beta_y^2 + \beta_z^2)^{1/2} \quad (7)$$

and

$$\beta_x = \beta_{xxx} + \beta_{xyy} + \beta_{xzz} \quad (8)$$

$$\beta_y = \beta_{yyy} + \beta_{xxy} + \beta_{yzz} \quad (9)$$

$$\beta_z = \beta_{zzz} + \beta_{xxz} + \beta_{yyz} \quad (10)$$

because the values of the polarizabilities ( $\alpha$ ) and hyperpolarizability ( $\beta$ ) from Gaussian 09W output are showed in atomic units (a.u), the measured values have been changed into electrostatic units (esu) ( $\alpha$ : 1a.u= 0.1482 x 10<sup>-12</sup>esu,  $\beta$ : 1 a.u = 8.6393×10<sup>-33</sup>esu). The total first hyperpolarizability of the title compound BS2M has been calculated to be 2.141X10<sup>-30</sup>esu as shown in Table 7.

Table-7: The electric dipole moment (D), average polarizability, first hyperpolarizability, etc., of Benzothiophene sulfone-2-methanol by B3LYP/6-311++G\*\*

$\mu$ and $\alpha$ components	B3LYP/6-311++G**	$\beta$ components	B3LYP/6-311++G**
$\mu_x$	-1.4686033	$\beta_{xxx}$	-181.5241
$\mu_y$	-0.0004406	$\beta_{xxy}$	-0.004541
$\mu_z$	-0.3606857	$\beta_{xyy}$	7.504349
$\mu$ (D)	2.287074	$\beta_{yyy}$	0.000248
$\alpha_{xx}$	138.2710834	$\beta_{xxz}$	41.58624
$\alpha_{xy}$	0.0314955	$\beta_{xyz}$	-0.01228
$\alpha_{yy}$	58.3914681	$\beta_{yyz}$	-7.794810
$\alpha_{xz}$	-23.6559949	$\beta_{xzz}$	-88.47132
$\alpha_{yz}$	-0.0015086	$\beta_{yzz}$	-0.072994
$\alpha_{zz}$	154.7665788	$\beta_{zzz}$	141.41629
$\Delta\alpha$	37.41515×10 <sup>-12</sup> esu		
$\alpha$ (esu)	17.360599×10 <sup>-12</sup> esu	$\beta$ total (esu)	2.141 ×10 <sup>-30</sup> esu

## 8. Molecular Electrostatic Potential Maps (MESP)

The molecular electrostatic potential map (MESP) was obtained by mapping of molecular electrostatic potential (MEP)  $V(r)$  on the iso-electron density surface of a molecule. The MEP, at any taken point  $r(x,y,z)$  is the sum of two opposing interaction energies positive and negative. The molecular electrostatic potential (MESP) of  $V(r)$  at a point  $r$  with nuclear charges  $\{Z_A\}$  pointed at  $\{R_A\}$  and the electron density  $\rho(r)$  is represented in the following equation.

$$V(r) = \sum_A^N [(Z_A / |r-R_A|) - \int \rho(r') d3r' / |r-r'|] \quad (11)$$

Here,  $N$  indicates the total number of nuclei in the molecule and the two terms refer to the nuclear potential and the electronic contributions within the molecule respectively. The combination of these two parameters represents about the appreciable conjugation of electron-rich i.e. nucleophilic regions in the compound under investigated. The MESP topography of the molecular system was mapped by examining the Eigen value of the Hessian matrix at the point where the gradient  $V(r)$  disappears. The electrostatic potential was a physical term of a titled molecule accompanied to show how a molecule was first “seen” or “felt” by another nearing group. A region in the molecule under investigation that has a negative electrostatic potential will be susceptible to electrophilic attack, If it has a more negative more will be attack. It was not as simple task to use electrostatic potentials to predict the nucleophilic attack. It was seen in Fig. 10 that, the negative charge red color indicates negative charge and blue color indicates positive charge is located over the oxygen atoms viz., the atoms O11, O12, O13, and positive charge is located over the benzene. These regions are the predicted centers of electrophilic and nucleophilic attack respectively.



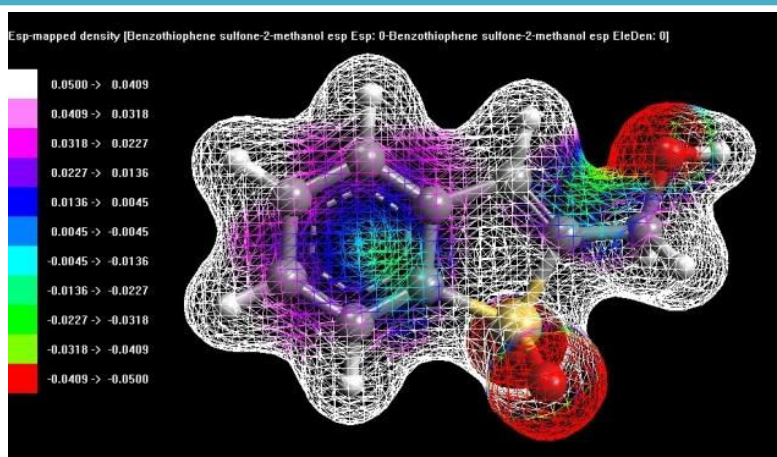


Figure-10: B3LYP/6-311++G\*\* calculated 3D molecular electrostatic potential maps of Benzothiophene sulfone-2-methanol.

## 9. Conclusions

The FT-IR spectra of the Benzothiophene sulfone-2-methanol have been recorded and the enumerated vibrational assignments are reported for the first time. Experimental geometry and harmonic vibrational wave numbers are reproduced excellently while we carry out the normal coordinate analysis on BS2M. It was observed that there was a good coincidence between the crystal structure data and optimized structure data. All most all fundamental vibrations display very small deviations when the computed and measured wave numbers are compared. NBO analysis was performed and it gives information about the intramolecular charge transfer between the bonding and antibonding orbitals. The UV-Vis spectra of the titled compound was recorded in the region 200-800 nm and reported the observed  $\lambda_{\max}$  at which is good agreement with the theoretically calculated value by using TDDFT method. The fluorescence spectra at different wavelengths have been studied and it indicates the red shift of the  $\lambda_{\max}$ .

## 10. Acknowledgement

The corresponding author, A.Veeraiah is highly grateful to Science and Engineering Research Board, Department of Science and Technology, Government of India (Project code- SB/EMEQ/2014) and Management D. N. R. College Association for their financial support and cooperation respectively. The second author, K. Anand Soloman thanks the management of Dayananda Sagar University for the financial support and encouragement. Further, the authors are highly grateful to Prof. T. Sundius for Molvib program.

## References

1. Arivazhagan, M., Rexalin, D. A., and Ilango, G. 2014; DFT analysis of P-nitrobenzotrifluoride--a combined study of experimental (FT-IR and FT-Raman) and theoretical calculations, *SpectrochimicaActa* part A, volume 121: 641-649.
2. Becke, A. D. 1988; Density-functional exchange-energy approximation with correct asymptotic behavior, *PHYSICAL REVIEW A*, volume 38, No. 6: 3098.
3. Cadoni, E., Ferino, G., pitzanti, P., Secci, F., Fattuoni, C., Nicolo, F., and Bruno, G. 2014; Halogen and Hydrogen Bonding Benzothiophene Diol Derivatives: A Study Using ab initio Calculations and X-Ray Crystal Structure Measurements, *chemistry open*, volume 4, No. 2: 161-168.





4. Ellis, B., Griffiths, P. J. F. 1966; The ultra-violet spectra of some heterocyclic thioamides and hydrogen bonding, *Spectrochimica Acta*, volume 22, No.12: 2005-2032.
5. Frisch, M. J. et al., GAUSSIAN09, Revision A.02, Gaussian Inc., Wallingford, CT, 2009.
6. Lee, C., Yang, W. and Parr, R. G. 1988; Development of the Colle-Salvetti correlation-energy formula into a functional of the electron density, *PHYSICAL REVIEW B*, Volume 37 NO.2: 785-789.
7. Ramalingam, S., Anbusrinivasan, P. and Periandy, S. 2011; FT-IR and FT-Raman spectral investigation, computed IR intensity and Raman activity analysis and frequency estimation analysis on 4-chloro-2-bromoacetophenone using HF and DFT calculations, *Spectrochimica Acta Part A*, volume 78, No.2, 826-834.
8. Roy Dennington, Todd A. Keith, and John M. Millam, GaussView, Version 6, Semichem Inc., Shawnee Mission, KS, 2016.
9. Sundius, T., 1990, 218, 321. MOLVIB: A Program for Harmonic Force Field Calculations, *J. Mol. Struct.*, QCPE program No. 604 (1991).
10. Varsanyi, G. 1974; Assignments for Vibrational Spectra of Seven Hundred Benzene Derivatives, vols. 1 and 2, Adam Hilger.